Clay−Organosiloxane Hybrids: A Route to Cross-Linked Clay Particles and Clay Monoliths

Athanasios B. Bourlinos, David D. Jiang, and Emmanuel P. Giannelis*

Department of Materials Science and Engineering, Cornell University, Ithaca, New York 14853

Received January 2, 2004. Revised Manuscript Received April 12, 2004

Reaction of bis(trimethoxysilyl)hexane, $(CH_3O)_3Si(CH_2)_6Si(OCH_3)_3$, and the protonated salt of 3-aminopropyltriethoxysilane, $(C_2H_5O)_3Si(CH_2)_3NH_3^+Cl^-$, with different clay aqueous colloidal dispersions produces a network of clay platelets cross-linked on their edges by the corresponding organosiloxanes. In the case of the α,ω-bridging organosiloxane, where the surface modification of the clay by the silane proceeds on its outer surfaces, cross-linking results in a gel network that extends to the whole volume of the initial aqueous dispersion. Drying of this gel and grinding of the as-formed, relatively hard specimens affords fine hybrid powders consisting of cross-linked clay particles that inherit the swelling, intercalation, and ion-exchange properties of the starting clay. Controlling both the composition of the initial suspension (clay type, solvent, and concentration) and the drying process, enables the fabrication of monolithic clay hybrids. In the case of the protonated aminosiloxane, the surface modification of the clay takes place both within its interlayer space and at its edges. The former leads to the formation of silsequioxane pillars within the clay galleries. The latter produces stiff yet ductile monoliths upon drying via condensation of edge-modified adjacent clay layers. When Laponite and $(CH_3O)_3Si(CH_2)_3N(CH_3)_3^+Cl^-$ are used, optically transparent monoliths (or clay glasses) are obtained.

Introduction

Clay minerals, synthetic or natural, are an important, plentiful, and low-cost class of materials with unique swelling, intercalation, and ion-exchange properties. Their thermal stability, chemical inertness, and laminate structure make them suitable for numerous applications involving particle engineering processes, such as creation of porosity (pillared clays),[1] dispersion in polymer matrixes for reinforcing purposes (clay−polymer nanocomposites),[2] shape fabrication of ultralight clay materials (clay hollow matter),[3] film deposition on substrates for protecting, insulating, and sensing purposes (clay coatings and clay modified surfaces),[4,5] and manufacture of clay objects (clay ceramics).[6,7]

In addition to these attractive features, clay minerals also exhibit a wide surface chemistry that takes place at their layers' edges, including surface modification through ion-exchange reactions and chemical modification with organosilanes (organochlorosilanes and organosiloxanes). In the first case, the presence of cation exchange sites at the edges (∼10% of the total cation exchange capacity of the mineral) offers an easy route for accommodating charged entities with specific functionalities. In the second case, the organosilane is attached to the clay edges through condensation reactions between the surface hydroxyl groups and the chloro- or alkoxy- groups of the organosilane, thus affording Si−O−Si or Al−O−Al covalent bonds.[8,9] Although the content of these −OH groups is low, and so is the amount of the grafted organosilane,[10] the particular postsynthetic route generally leads to an effective alteration of the clay properties, for instance, of its miscibility with organic solvents and polymers[9] and of its interlayer chemistry.[11,12]

The edge chemistry of the clays is crucial for their fabrication into ceramics of various engineering forms, e.g., films or macroscopic objects. In these processes, the cross-linking of adjacent clay particles is critical to getting hard, stiff ,and relatively ductile ceramics instead of cracked monoliths or films or powder aggregates. Two routes are generally used. In the first and well-known procedure, an aqueous clay slurry plus all additives are cast into a mold, thus affording a well-shaped object after water removal. Calcination at high temperatures promotes sintering between the clay primary particles and the additive(s), densifying into a shaped network.[6] The second procedure exploits the

* To whom correspondence should be addressed. Phone: 607-255-9680. Fax: 607-255-2365. E-mail: epg2@cornell.edu.

(1) Mitchel, I. V. In *Pillared Layered Structures. Current Trends and Applications*; Elsevier: London, 1990.
(2) Giannelis, E. P. *Adv. Mater.* **1996**, *8* (1), 29.
(3) Bourlinos, A. B.; Karakassides, M. A.; Petridis, D. *Chem. Commun.* **2001**, *16*, 1518.
(4) Nadeau, P. H. *Appl. Clay Sci.* **1987**, *2*, 83.
(5) Coche-Guérente, L.; Cosnier, S.; Desprez, V.; Labbé, P.; Petridis, D. *J. Electroanal. Chem.* **1996**, *401*, 253.
(6) Moya-Jose, S. *Adv. Mater.* **1995**, *7* (2), 185.
(7) Isayama, M.; Kunitake, T. *Adv. Mater.* **1994**, *6* (1), 77.
(8) Song, K.; Sandi, G. *Clays Clay Miner.* **2001**, *49*, 119.
(9) Carrado, K. A.; Xu, L.; Csencsits, R.; Muntean, J. V. *Chem. Mater.* **2001**, *13*, 3766.
(10) Rausell-Colom, J. A.; Serratosa, J. M. In *Chemistry of Clays and Clay Minerals*; Newman, A. C. D., Ed.; Wiley-Interscience: New York, 1987; p 371.
(11) Wasserman, S. R.; Soderholm, L.; Staub, U. *Chem. Mater.* **1998**, *10*, 559.
(12) Giaquinta, D. M.; Soderholm, L.; Yuchs, S. E.; Wasserman, S. R. *Radiochim. Acta* **1997**, *76*, 113.

10.1021/cm049975z CCC: $27.50
Published on Web 05/19/2004

chemical reactivity of the Si−OH or Al−OH groups present at the clay edges toward bridging modifiers. This method proceeds at ambient conditions and is mainly associated with the manufacture of layered ceramic films. For example, addition of H_3PO_4 in a clay aqueous colloidal dispersion, followed by spreading of the slurry over a substrate and drying, leads to esterification reactions between the acid and the edge −OH groups among adjacent layers, thus affording dense films with high resistance against aqueous "etching".[7] Such a cross-linking process offers a soft route for the fabrication of molecularly modified clay ceramics consisting of interconnected clay particles.[7]

In an attempt to find new, soft chemistry cross-linking approaches for fabricating clay ceramics with interesting properties, the present work describes how surface modification of clay minerals with functional organosiloxanes can lead to shaped networks of interconnected clay particles, or, in other words, to hybrid clay monoliths. Two different kinds of organosiloxanes were employed for this purpose. The first is bis(trimethoxysilyl)hexane, $(CH_3O)_3Si(CH_2)_6Si(OCH_3)_3$, an α,ω bridging organosiloxane, which has already been used to synthesize silsequioxane clusters, porous gels, and intriguing periodic mesostructures.[13−15] The other type is either the protonated 3-aminotriethoxysilane $(C_2H_5O)_3Si(CH_2)_3NH_3^+Cl^-$, or the quaternary ammonium organosiloxane $(CH_3O)_3Si(CH_2)_3N(CH_3)_3^+Cl^-$. The use of the latter in pillaring clays has already been exploited.[16] Ion-exchange of Laponite particles with the quaternary ammonium organosilane under controlled conditions is of particular interest because it leads to highly transparent Laponite monoliths, thus providing for the first time optically transparent clay-based hybrids.

Experimental Section

Materials. The clays used in this work were a synthetic hectorite (Laponite RD, Laport), a natural montmorillonite (Nanocor), and a fluorohectorite (Corning, Inc.). All clays were sodium saturated before use. Bis(trimethoxysilyl)hexane, $(CH_3O)_3Si(CH_2)_6Si(OCH_3)_3$, and $(CH_3O)_3Si(CH_2)_3N(CH_3)_3^+Cl^-$, were purchased from Gelest, and 3-aminopropyltriethoxysilane, $(C_2H_5O)_3Si(CH_2)_3NH_2$, was purchased from Aldrich. Rhodamine B and methylene blue dyes were supplied by Aldrich and Fluka, respectively. Formamide (Fisher Chemicals), *N*,*N*-dimethylformamide (DMF, Fisher Chemicals), and tetrahydrofuran (THF, Mallinckrodt) were used as received.

Methods. *Clay−$(CH_3O)_3Si(CH_2)_6Si(OCH_3)_3$ Hybrids.* Sodium clay (0.5 g) was dispersed in 20 mL of H_2O, and 0.5 g of the α,ω organosiloxane was added. The mixture was allowed to stir at room temperature for 24 h during which a gel occupying the whole volume of the initial aqueous dispersion was formed. The gel was spread on a glass plate and dried at 60 °C for 24 h. The as-formed hard specimens were ground into a fine powder for further analysis. LAP2SI6, NAN2SI6, and FHC2SI6 refer to Laponite, montmorillonite, and fluorohectorite hybrids, respectively.

Clay monoliths were prepared as above by properly adjusting the sol concentration and selecting the right solvent. More specifically, for the LAP2SI6 and FHC2SI6 cases, 0.5 g of the corresponding clay was first dispersed in 4 mL of H_2O followed by the addition of 1 mL of DMF for LAP2SI6 or THF for FHC2SI6 containing 0.5 g $(CH_3O)_3Si(CH_2)_6Si(OCH_3)_3$. The slurries were sonicated until gelation. The gels were aged for 10 days at room temperature, vacuum-dried at ambient conditions for 24 h, and finally dried at 60 °C for an additional 24 h. For the NAN2SI6 case, 0.5 g of montmorillonite was first dispersed in 6 mL of H_2O, and 4 mL of $HCONH_2$ containing 0.5 g of siloxane was added. The slurry was treated as above except drying at 60 °C was for 4 days.

Clay−$^+H_3N(CH_2)_3Si(OC_2H_5)_3$ Hybrids. A 3-g portion of clay was dispersed in 100 mL of H_2O, and 50 mL of H_2O containing 3 g of $(C_2H_5O)_3Si(CH_2)_3NH_2$ acidified with an equimolar amount of HCl was added. Instantly, flocculation of the clay particles took place. After the slurry was stirred at room temperature for 24 h it was filtered under vacuum. After repeating washings with water, the clay paste was dried at room temperature. During drying, the clay paste continuously shrank while maintaining its original shape, producing a dry, stiff monolith. By this method, it was possible to fabricate the montmorillonite and fluorohectorite based monoliths but not the Laponite analogue. The latter tends to crack after drying. The as-prepared monoliths are designated as NANSIAM and FHCSIAM, respectively.

Optically Transparent Laponite Monoliths. Sodium Laponite RD (0.5 g) was first dispersed in 15 mL water, followed by the addition of 10 mL of formamide containing 1 g of a 50% methanolic solution of $(CH_3O)_3Si(CH_2)_3N(CH_3)_3^+Cl^-$. A viscous suspension formed immediately. After stirring for 24 h at ambient temperature, the sample was vacuum filtered, dried for 3 days at room temperature and then at 65 °C for 10 h, to finally produce a highly transparent monolith. The same procedure was also used for the fabrication of colored monoliths, except that 1 mL of a 0.02%w/v rhodamine B or methylene blue aqueous solution was also added to the formamide/organosiloxane mixture.

A drawing of the different fabrication approaches is shown in Scheme 1.

Characterization. XRD analysis was carried out on a Scintag PAD X diffractometer using Cu Kα radiation (λ = 1.54Å) and 2°/min scan rate. TGA measurements were obtained on a Seiko Instruments TG/DTA 320 model analyzer. The samples were measured against an alumina standard in a 40 mL/min N_2 flow with a temperature ramp of 20 °C/min to 600 °C. IR measurements were made on a Mattson Instruments 2020 Galaxy Series FT-IR using KBr pellets. Bright field TEM images were obtained at 120 kV with a JEOL JEM-1200EX electron microscope. SEM images were obtained on a Leica 440 microscope. Compression moduli were measured using a Starrett durometer.

Results and Discussion

To examine the effect of the layer dimensions on the cross-linking processes and the fabrication of monoliths, three clay sources with different layer sizes of 50 nm (Laponite), 200 nm (montmorillonite), and >1000 nm (fluorohectorite) were employed. In addition to differences in size, the edge octahedral hydroxyl groups in fluorohectorite are replaced by the more chemically inert fluorine.[17] Figure 1, left, depicts the XRD patterns of the corresponding sodium-saturated clays. The line widths of the (001) reflections become sharper as we move from Laponite to fluorohectorite suggesting the presence of progressively larger and better-organized clay particles.

(13) Loy, D. A.; Carpenter, J. P.; Alam, T. M.; Shaltout, R.; Dorhout, P. K.; Greaves, J.; Small, J. H.; Shea, K. J. *J. Am. Chem. Soc.* **1999**, *121*, 5413.

(14) Boury, B.; Chevalier, P.; Corriu, R. J. P.; Delord, P.; Moreau, J. J. E.; Chiman, M. W. *Chem. Mater.* **1999**, *11*, 281.

(15) Asefa, T.; Yoshina-Ishii, C.; MacLachlan, M. J.; Ozin, G. A. *J. Mater. Chem.* **2000**, *10*, 1751.

(16) Szabó, A.; Gournis, D.; Karakassides, M. A.; Petridis, D. *Chem. Mater.* **1998**, *10*, 639.

(17) Breu, J.; Stoll, A.; Lange, K. G.; Probst, T. *Phys. Chem. Chem. Phys.* **2001**, *3*, 1232.

Scheme 1. Schematic of the Different Fabrication Approaches: Clay−$(CH_3O)_3Si(CH_2)_6Si(OCH_3)_3$ (A), Clay−$^+H_3N(CH_2)_3Si(OC_2H_5)_3$ (B), and Optically Transparent Laponite Monoliths (C)

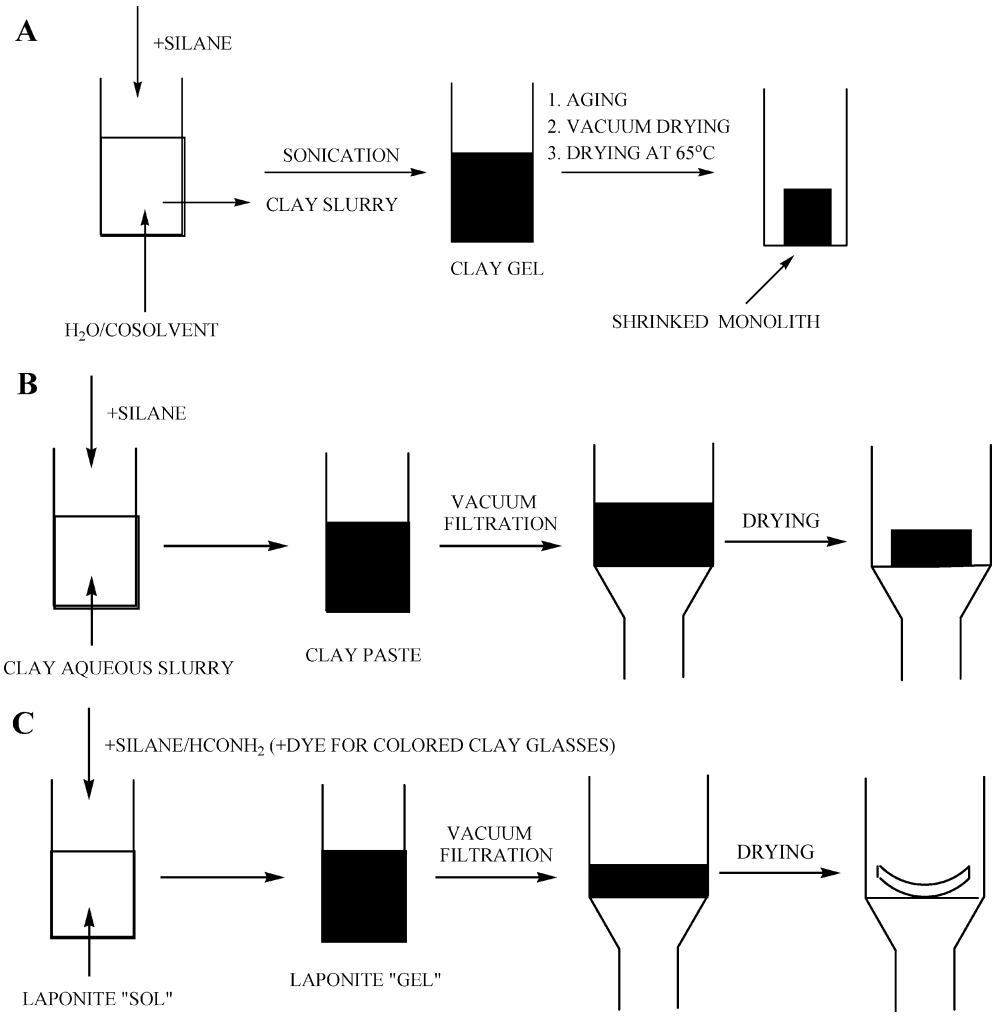

Clay−$(CH_3O)_3Si(CH_2)_6Si(OCH_3)_3$ Hybrids. Figure 1, right, presents the XRD patterns of the LAP2SI6, NAN2SI6, and FHC2SI6 powdered samples. The Laponite derivative is highly amorphous, whereas the hybrids based on montmorillonite and fluorohectorite exhibit a peak at 10 and 12.5 Å, respectively. These results suggest that surface modification by the organosiloxane proceeds on the outer surfaces of the minerals and not within their interlayer space. The peak broadening of the hybrids compared to the neat clays also suggests that surface modification induces a stacking disorder in the clay particles. The collapsed spacing observed for NAN2SI6 is due to dehydration and reversible migration of the sodium ions to the hexagonal cavities of the tetrahedral silicate sheets upon thermal drying.[18] However, no collapse was observed for the fluorohectorite layers after the same treatment. Indeed, control experiments with the parent clays revealed that, in contrast to montmorillonite, fluorohectorite retains its *d* spacing even after calcination at 550 °C in air.

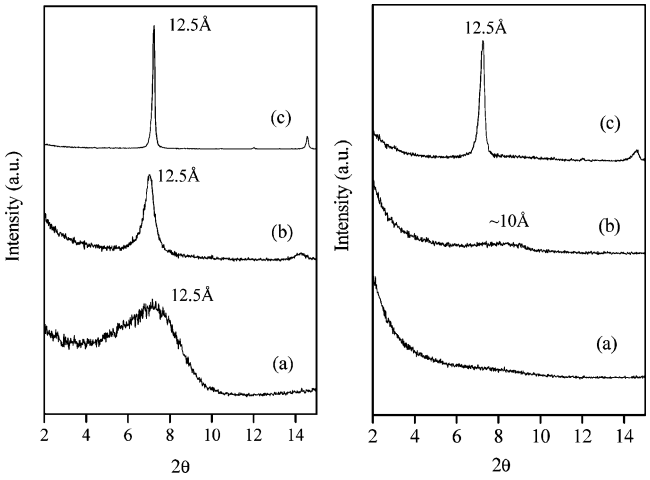

Figure 1. Left: XRD patterns of sodic Laponite (a), montmorillonite (b), and fluorohectorite (c). Right: XRD patterns of the LAP2SI6 (a), NAN2SI6 (b), and FHC2SI6 (c) powders.

We suspect that the surface modification involves hydrolysis of the methoxy groups of the organosilane to silanol groups and condensation with the surface hydroxyl groups located at the edges of the clay layers (fluorohectorite still possesses a small amount of −OH groups at the edges of the tetrahedral layer[17]). The bifunctionality of the organosiloxane offers the possibility to attach one end of the organosiloxane to one particle and the other end to another neighboring particle. In this way, the gelation of the clay slurries upon addition of the organosiloxane can be easily

(18) Karakassides, M. A.; Madejová, J.; Arvaiová, B.; Bourlinos, A.; Petridis, D.; Komadel, P. *J. Mater. Chem.* **1999**, *9*, 1553.

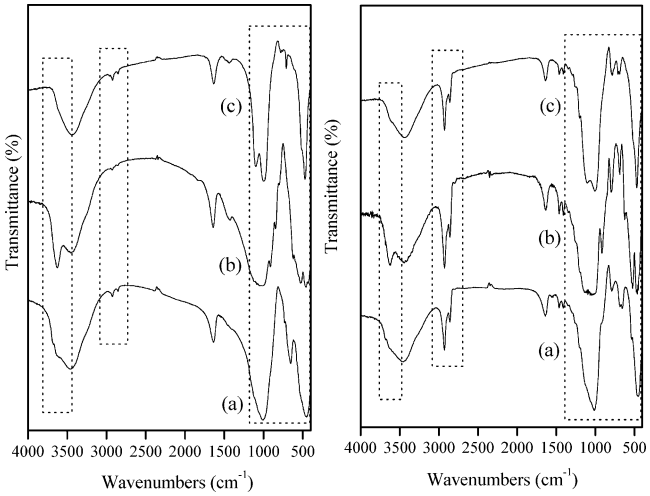

Figure 2. Left: IR spectra of sodic Laponite (a), montmorillonite (b), and fluorohectorite (c). Right: IR spectra of LAP2SI6 (a), NAN2SI6 (b), and FHC2SI6 (c).

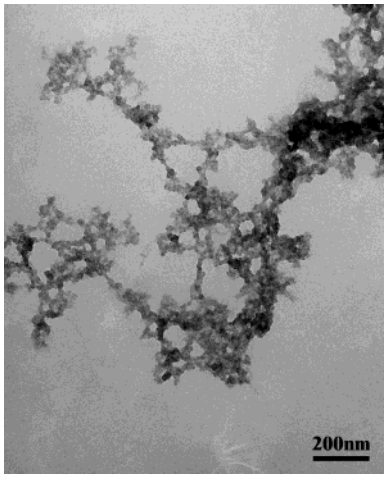

Figure 3. TEM image of the LAP2SI6 sample.

rationalized by the formation of a network consisting of clay layers interconnected at their edges by the organosiloxane with water molecules trapped within the gel network. Note that the gelation time decreases and the gel stiffness increases with increased layer dimensions.

Several pieces of evidence support the above-mentioned mechanism. First, the organosiloxane by itself does not gel in water. It forms instead oil droplets and remains unreacted even after 24 h stirring in water. Second, no gelation occurs when the ethoxy instead of methoxy organosiloxane derivative is used. This can be attributed to the slower hydrolysis rate of the ethoxy versus the methoxy groups. Third, protecting the edge −OH groups via trimethylsilylation capping[8,19] does not lead to gelation upon addition of the organosiloxane. Last, trimethoxysilylhexane, $(CH_3O)_3Si(CH_2)_5CH_3$, instead of the α,ω bridging organosiloxane, also does not form a gel. These observations clearly point to the bridging of neighboring particles by the α,ω-organosilane as the gel-forming mechanism.

It is important to note that changing the organic spacer from six to two carbon atoms [i.e., $(CH_3O)_3Si(CH_2)_2Si(OCH_3)_3$] still leads to gelation with Laponite and montmorillonite, but not with fluorohectorite. However, in contrast to the hexane spacer, the gelation time increases with increased layer lateral dimensions. The gelation times are higher than those observed for the hexane-linked organosiloxane, probably due to the rigidity of the ethane spacer, which in turn reduces the flexibility of the trialkoxysilyl ends toward condensation.[20] The inflexibility in conjunction with spatial restrictions imposed from the larger and larger layer dimensions might contribute to the slower gelation times.

Figure 2 shows the IR spectra of LAP2SI6, NAN2SI6, and FHC2SI6. For comparison, the spectra of the pristine clay are also included. The hybrids exhibit strong absorption bands below 3000 cm^{-1} and weaker absorptions between 1400 and 1500 cm^{-1}, attributed to the $-CH_2-$ groups of the grafted siloxane. In addition, the absorption bands in the low region spectra (1000−500 cm^{-1}) become more distinct than those present in the pristine clays. These peaks can be assigned to the Si−O groups of the clay framework and grafted organosiloxane.[13,18] No changes are observed above 3500 cm^{-1}, where typically the −OH stretching vibration appears. The −OH groups that are buried within the layered framework overwhelm the number of edge-located groups. Therefore, any modification of the edge −OH groups by the organosiloxane cannot be followed by changes of the band at ∼3500 cm^{-1}. It is interesting to note that the relative intensities of the bands at ∼1000 cm^{-1} and ∼500 cm^{-1}, assigned to the Si−O vibrations of the clay framework, remain unchanged before and after modification with the bridging organosiloxane, suggesting the absence of silica particles (see below). However, we cannot exclude the presence of oligomeric species in addition to molecular bridges between the clay particles.

The TGA trace of the NAN2SI6 hybrid exhibits two weight losses:[21] one near 100 °C due to surface absorbed water (3%), and another one in the region 400−600 °C due to the oxidation of the hybrid's organic content. The organic content is 13% for NAN2SI6, and, in general, ∼15% for all hybrids. Assuming an average formula of $(O)_{1.5}Si(CH_2)_6Si(O)_{1.5}$ for the grafted organosiloxane in the hybrids[14,20] and taking into consideration their organic content (∼15%), we conclude that the hybrid solids are composed of 70% clay and 30% grafted organosiloxane. Interestingly, a physical mixture of clay, e.g. montmorillonite, and silica hybrid xeropowder, the latter derived from acid hydrolysis of the $(CH_3O)_3Si(CH_2)_6Si(OCH_3)_3$ in water, in a mass ratio of 70:30, reveals enhanced intensity of the band at ∼1000 cm^{-1} at the expense of that at ∼500 cm^{-1} mainly because the silica hybrid powder, in contrast to the clay, exhibits a very strong absorption band at ∼1000 cm^{-1} and a very weak one at ∼500 cm^{-1} supporting our assertion about the absence of silica particles.

A TEM image of LAP2SI6 is shown in Figure 3. In contrast to the unmodified clay, where individual clay particles with a lateral size of ∼50 nm are present, a

(19) Kikuta, K.; Ohta, K.; Takagi, K. *Chem. Mater.* **2002**, *14*, 3123.
(20) Boury, B.; Corriu, R. J. P.; Le Strat, V. *Chem. Mater.* **1999**, *11*, 2796.
(21) Carrado, K. A.; Thiyagarajan, P.; Song, K. *Clay Miner.* **1997**, *32*, 29.

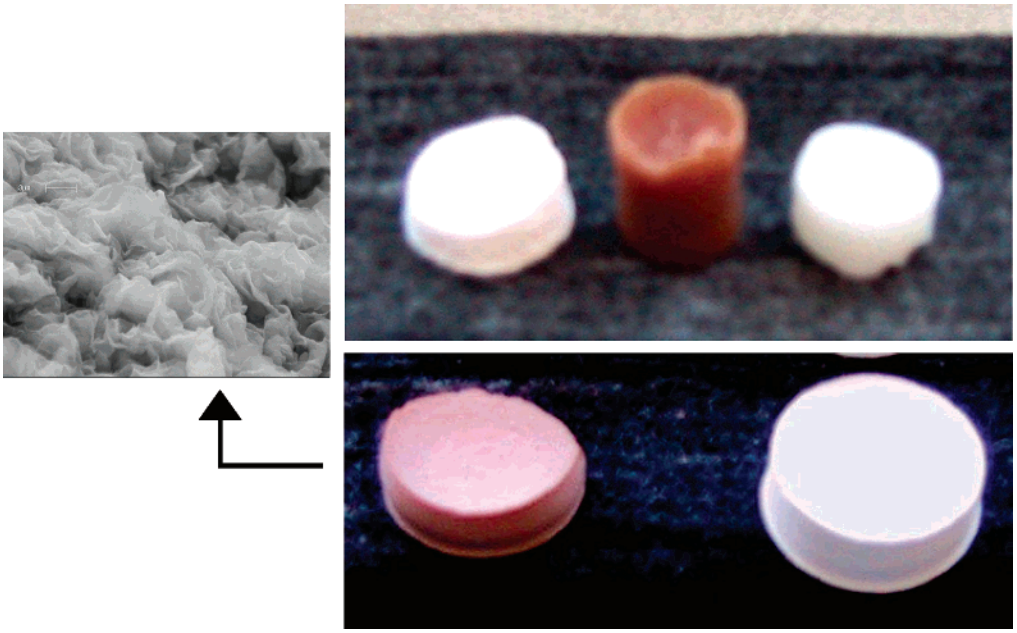

Figure 4. Top: Photo depicting well-shaped monolithic clay objects of LAP2SI6 (right), NAN2SI6 (middle), and FHC2SI6 (left). Bottom: Photo depicting monoliths of NANSIAM (left) and FHCSIAM (right). Aside: SEM image of NANSIAM sample.

strongly aggregated morphology appears for the hybrids as a result of particle bridging by the organosilane.

The cross-linked hybrids do not disperse, but instead they swell in water. In addition, they are accessible for ion-exchange reactions. Characteristically, ion-exchange of the Na^+ ions for $C_{12}H_{25}PPh_3^+$ leads instantly to organoclay hybrid derivatives with $d_{001} = 35$ Å and IR bands characteristic for the aromatic groups of the ion-exchanged organocation (above 3000 cm^{-1} and in the region 1500−1600 cm^{-1}).

Whereas bridging by the organosilane is ubiquitous in all hybrid systems, monoliths were obtained only for limited concentrations and solvents. Sol concentration and the nature of solvent are crucial in minimizing internal stresses during drying.[22] Specifically, to get crack free monoliths (Figure 4, top) different conditions were used for each clay type. For LAP2SI6 (10% w/v), NAN2SI6 (5% w/v), and FHC2SI6 (10% w/v), the presence of 20% DMF, 40% $HCONH_2$, and 20% THF, respectively, in the suspensions ensured the presence of crack-free monoliths (the numbers in parentheses denote the concentration of each clay slurry, while the clay to organosiloxane mass ratio was maintained at 1).

Clay−$^+H_3N(CH_2)_3Si(OC_2H_5)_3$ Hybrids. Aminofunctional silanes of the $(RO)_3Si(CH_2)_3NH_2$ type have been used as precursors to form silica pillared clays.[16,23,24] Protonation of the amine group charges positively the aminosiloxane, which then can be easily inserted into the clay interlayers where condensation reactions between the monomeric entities form oligomeric silsequioxane pillars. We became interested in transforming these pillared hybrids into a monolith. In an envisioned application, pillared clay monoliths could serve as unique porous ceramics for molecular sieving processes. A similar concept has been demonstrated already for mesoporous silica monoliths.[25]

We have developed a fast and simple method to form these monoliths. The method consists of mixing a clay suspension with an aqueous solution of the protonated aminosiloxane (ethoxy form), stirring the mixture at ambient temperature for 24 h, followed by vacuum filtration, washing of the hybrids, and drying. Typical images of the NANSIAM and FHCSIAM monoliths are shown in Figure 4, bottom. (The method does not work well for Laponite). SEM images confirm their compact structure and the absence of macropores or cracking in the monoliths (see Figure 4).

The XRD patterns of LAPSIAM, NANSIAM, and FHCSIAM exhibit d_{001} values in the range 16−17 Å, consistent with well-washed silsequioxane pillared structures[16] (Figure 5). As expected, the diffraction peak becomes sharper as the layer size increases from Laponite to montmorillonite to fluorohectorite. Characteristically, the IR spectra of the pillared samples exhibit a broad band at ∼3000 cm^{-1} and two sharper bands between 1500 and 1600 cm^{-1}, assigned to the $-NH_3^+$ stretching and bending vibrations, respectively (Figure 5). Furthermore, the organic content of these materials from the weight loss of the samples above 300 °C by TGA is ∼5%. Assuming an idealized formula of $(O)_{1.5}Si(CH_2)_3NH_3^+$ for the aminosiloxane,[16] we conclude that the particular samples are composed of 90% clay and 10% aminosilane. (Note that the organic ratio of the aminosilane is 0.53.)

Clay minerals possess part of their cation exchange capacity (∼10%) at their layer edges, the latter being easily accessible by charged species. Monolithic gels are obtained through clay particle bridging by the organosilane via electrostatic interactions of the protonated amino group on one end and condensation of the hydrolyzable ethoxy groups with another organosilane

(22) Brinker, C. J.; Scherer, G. W. In *Sol−Gel Science: The Physics and Chemistry of Sol−Gel Processing*; Academic Press: San Diego, CA, 1996.

(23) Fetter, G.; Tichit, D.; Massiami, P.; Durartre, R.; Figueras, F. *Clays Clay Miner.* **1994**, *42*, 161.

(24) Uchida, Y.; Nobu, Y.-I.; Momiji, I.; Matsui, K. *J. Sol-Gel Sci Technol.* **2000**, *19*, 705.

(25) Yang, H.; Shi, Q.; Tian, B.; Xie, S.; Zhang, F.; Yan, Y.; Tu, B.; Zhao, D. *Chem. Mater.* **2003**, *15*, 536.

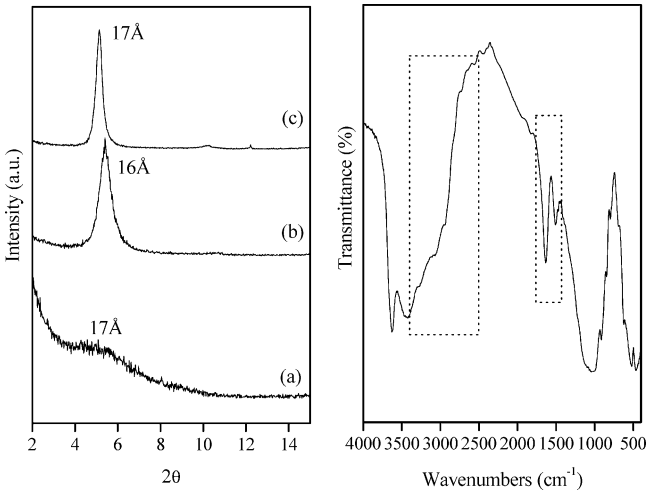

Figure 5. Left: XRD patterns of LAPSIAM (a), NANSIAM (b), and FHCSIAM (c). Right: IR spectrum of NANSIAM.

Table 1. Dimensions and Compression Moduli of the Monoliths

monolith	*d* (cm)	h_o (cm)	*E* (MPa)
LAP2SI6	1.2	0.7	6
NAN2SI6	1	1.2	8
FHC2SI6	1.4	0.5	4
NANSIAM	2	0.6	16
FHCSIAM	2	0.7	8

on the other. Note that $CH_3CH_2CH_2NH_3^+$, a nonhydrolyzable compound, did not produce a clay monolith.

Compression Modulus. The compression modulus, *E*, of each monolithic sample was derived from the slope of a standard stress (σ) versus strain (ϵ) curve.[26] Table 1 summarizes the dimensions (diameter, height, or thickness) and compression moduli of the above-discussed monolithic samples. It appears that the bonding interactions between neighboring clay particles (or otherwise the degree of cross-linking) and thus the modulus, are greater in the SIAM series than in the 2SI6, whereas, for a same series, the fluorohectorite derivatives appear to have the smaller bonding interactions as a result of the relatively smaller content of edge-located −OH groups.

Optically Transparent Laponite Monoliths. The fabrication of optically transparent Laponite monoliths is of particular value, as it demonstrates the first case of a clay glass. An aqueous dispersion of Laponite was treated for 24 h with $(CH_3O)_3Si(CH_2)_3N(CH_3)_3^+Cl^-$ in the presence of formamide to afford a viscous colloidal dispersion. Vacuum filtration of the slurry and drying of the filtrated gel led to a highly transparent Laponite monolith having a concave, lens-shape geometry (thickness 0.2 cm, diameter ∼2 cm) (Figure 6, left). Laponite was chosen because of its optical transparency and unique colloidal properties.[27] An aqueous dispersion of Laponite can be considered as a "sol", whereas the fractal aggregates that are formed upon bridging of the layers can be considered as a colloidal "gel".[27] From this point of view, the presented approach mimics a conventional sol−gel process.

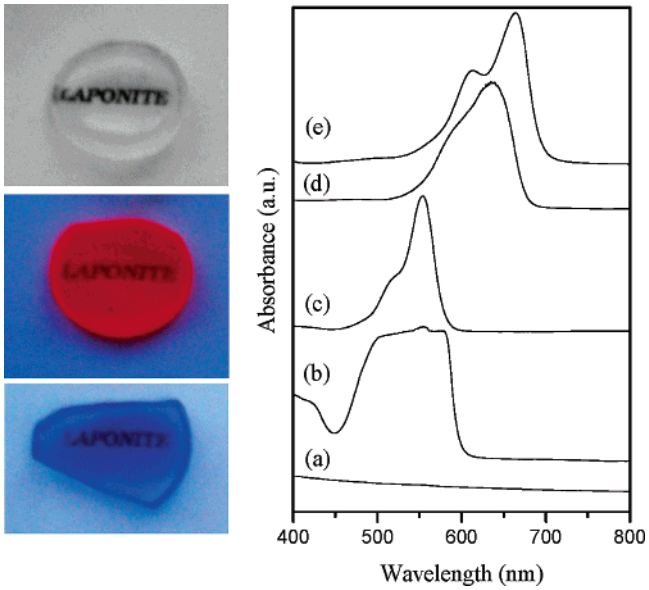

Figure 6. Left: Photographs of the Laponite-based monolithic specimens: as-prepared (colorless) and dye-doped (red, rhodamine B; blue, methylene blue). Right: Optical spectra of the un-doped (a) and dye-doped Laponite glasses (b, rhodamine B; d, methylene blue; and c and e, the absorption spectra of rhodamine B and methylene blue, respectively, in diluted aqueous solutions).

The method is strongly influenced by the solvent used. Water leads to opaque monoliths because of internal cracking caused during the drying process. In contrast, the use of formamide as a drying control solvent did allow the isolation of highly transparent monoliths. The hydrolyzable, positively charged organosiloxane plays an additional role in the stabilization of the monoliths. As stated above, once these molecules enter the interlayer space of clays through ion-exchange, they can afford silsequioxane pillared clay structures.[16] The XRD pattern of the as-modified Laponite sample shows a broad reflection with $d_{001} \approx 15$ Å, signaling the formation of a pillared Laponite structure (85% w/w in clay content based on TGA measurements). In contrast to the aminosilane used above, $(CH_3O)_3Si(CH_2)_3N(CH_3)_2(C_{18}H_{37})^+Cl^-$ or $(CH_3O)_3Si(CH_2)_3N(CH_3)(C_{10}H_{21})_2^+Cl^-$ led to opaque, fractured monoliths. These bulkier cations prevent effective interparticle bridging between Laponite particles.

The SEM profiles of the top (smooth) and cross-sectional (rough) surfaces of the Laponite monolith show its compact, crack-free microstructure, whereas the TEM image of the sample shows a dense packing of the Laponite particles within the monolithic framework (Figure 7). The lack of cracks or macropores in conjunction with the dense packing of the particles and their small size (50 nm) must be responsible for their optical transparency.

As-derived Laponite monoliths are colorless. Colored samples are obtained by adding a small amount of rhodamine B or methylene blue[28,29] in the suspension before gelation (Figure 6). Because of their positive charge, the dye molecules stick electrostatically to the

(26) Van Vlack, L. H. *Elements of Materials Science and Engineering*, 6th ed.; Addison-Wesley Publishing Company: Reading MA, 1989.
(27) Bonn, D.; Kellay, H.; Tanaka, H.; Wegdam, G.; Meunier, J. *Langmuir* **1999**, *15*, 7534.
(28) Arbeloa, F. L.; Martinez, J. M. H.; Arbeloa, T. L.; Arbeloa, I. L. *Langmuir* **1998**, *14*, 4566.
(29) Gessner, F.; Schmitt, C. C.; Neumann, M. G. *Langmuir* **1994**, *10*, 3749.

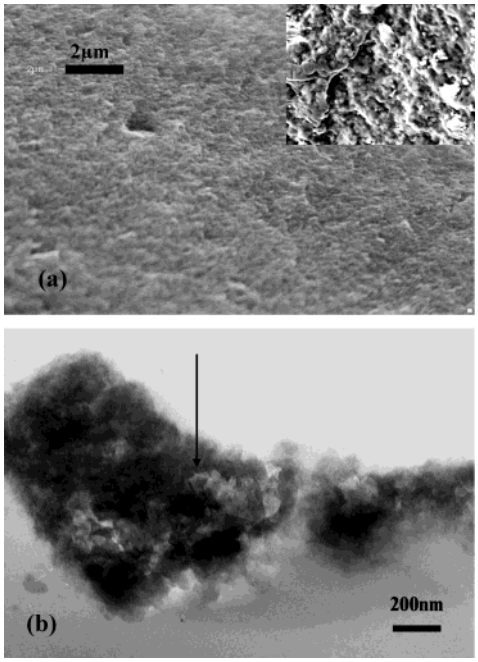

Figure 7. SEM images of the top and cross-sectional (inset) surfaces of the Laponite monolith (a), and the corresponding TEM image (b). The arrow indicates a Laponite particle.

Laponite layers, remaining behind after filtration. The optical properties of the monoliths are shown in Figure 6, right. Whereas the undoped Laponite glass is transparent, its colored derivatives exhibit strong absorption bands attributable to the corresponding dyes. The differences between the spectra in the solid and solution are attributed to the previously reported metachromatic effect.[28,29] The color of the samples is stable for at least one year.

Conclusions

Edge-surface modification of clay particles using α,ω bridging organosiloxane $(CH_3O)_3Si(CH_2)_6Si(OCH_3)_3$ and the protonated aminosiloxane $(C_2H_5O)_3Si(CH_2)_3NH_3^+$ or $(CH_3O)_3Si(CH_2)_3N(CH_3)_3^+Cl^-$ as modifiers leads to cross-linking of neighboring particles and enables the fabrication of monolithic objects under certain conditions by controlling the clay type, concentration, solvent, and drying process. This particular approach provides for the fabrication of a large variety of molecularly modified clay ceramics with intriguing properties at ambient conditions. The physical and mechanical properties of the monoliths could be tailored by changing the organic moiety of the organosilanes or the nature of the cross-linker. Monolithic derivatives that are optically transparent, hydrophobic, porous, etc., are possible. Because of its simplicity and effectiveness the same approach also could be applied to other oxide particles such as colloidal silica, alumina, titania, and iron oxide, among others.

Acknowledgment. This work was supported by AFOSR, the Cornell Center for Materials Research (CCMR) funded by NSR and ONR.

CM049975Z